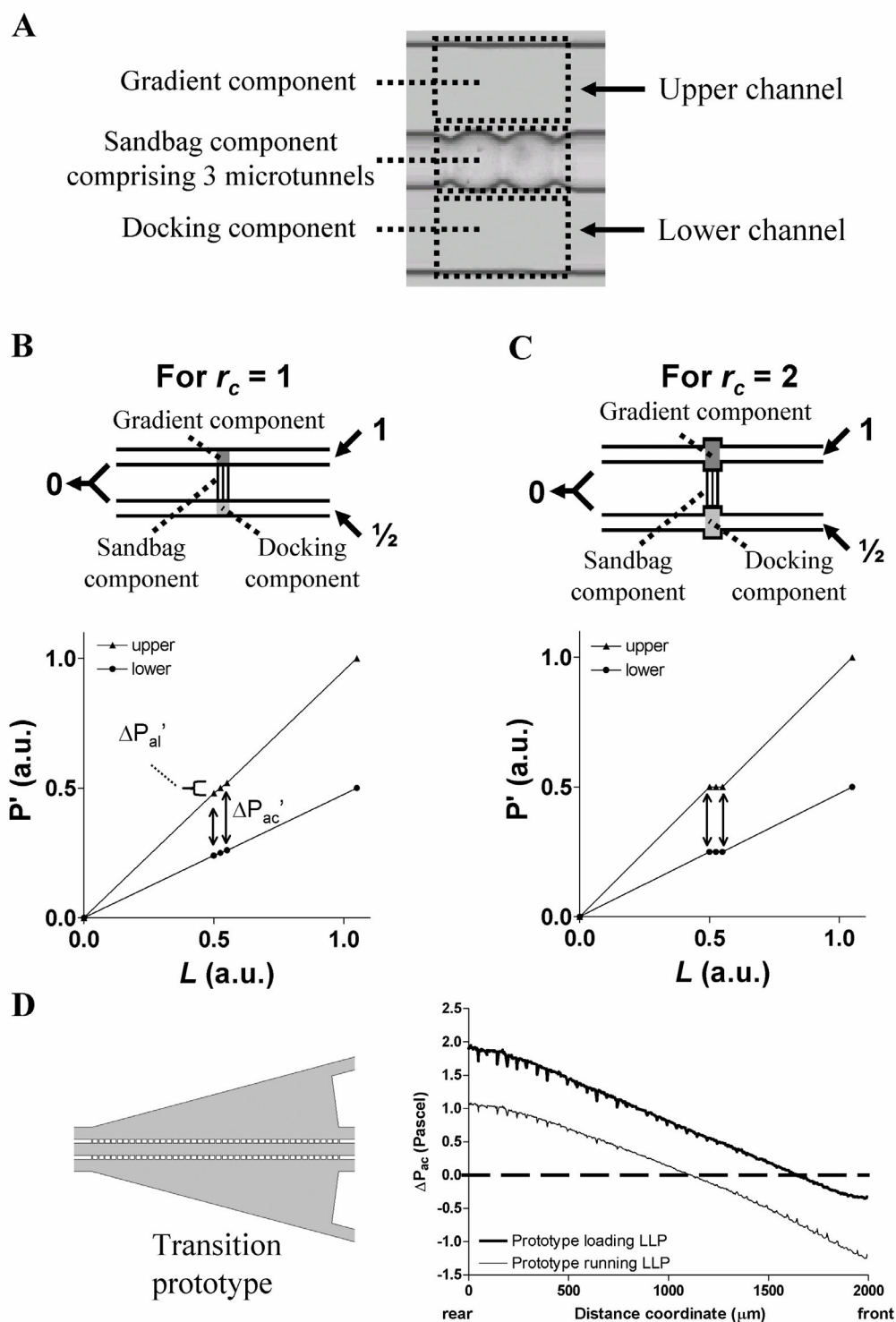


**Supplementary Figure 1: Effects of geometric modulation on fluidic pressure profile.**



To explain the geometric modulation on pressure profiles, a structural model was built with upper and lower microchannels separated by a “sandbag-like” structure called sandbag component (Supp-Fig 1A). The two channels were of circular cross-

sectional dimension and unit length. Sandbag component, positioned at the midway in the channel system, was comprised of 3 microtunnels that allowed cells to dock individually along the channel. Adjacent to the sandbag component are gradient and docking components, which were conceptual segments of the two channels. In order to illustrate the effects of geometric modulation, a partial enlargement was introduced by changing channel radii,  $r_c$ , of gradient and docking components (compare schematic models of Supp-Fig 1B & C). In both models, applied pressure was 1-fold higher in the upper (1 unit pressure) than the lower channel inlet (0.5 unit pressure) while flows were converged to a common outlet at zero pressure. Thus, fluidic flow from “right-to-left” along channel and “upper-to-lower” between channels were resulted due to the pressure differences introduced. Sandbag component was assumed to have high fluidic resistance such that negligible flow could pass through. With the above conditions, cell docking that was driven by pressure profiles of the two channels can be derived from the first principle of fluid dynamics<sup>1</sup>,

$$\Delta P' = \frac{Q}{r^4} L \quad (1)$$

where  $\Delta P'$  = pressure drop along channel divided by a constant,  $Q$  = flow rate,  $L$  = channel length and  $r$  = channel radius. As shown in Sup-Fig 1B & C, underneath each schematic model was the corresponding plot of “P’ vs  $L$ ” charts, where the  $\Delta P_{al}'$  ( $\Delta P'$  along microchannel) and  $\Delta P_{ac}'$  ( $\Delta P'$  across microchannels) values could be determined.

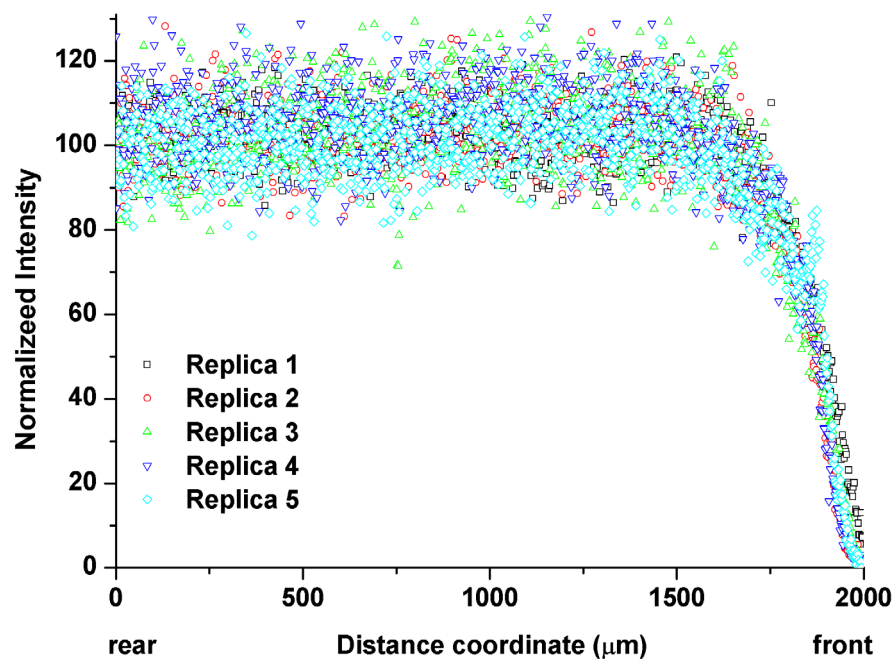
In accordance with Equation 1, increasing radius could proportionally reduce the  $\Delta P_{al}'$  values along gradient and docking components, given that these partially enlarged segments were short enough to maintain a constant overall flow rate. As illustrated,  $\Delta P_{ac}'$  values decreased more steeply for  $r_c = 1$  (Supp-Fig 1B, chart) than  $r_c = 2$  (Supp-Fig 1C, chart) along sandbag positions. A stable and constant pressure difference was achieved by modulating the slope of pressure profiles with 1-fold radii increment at gradient and docking components. This simple geometric modulation suggests the possibility to maintain a constant  $\Delta P_{ac}'$  that is important to immobilize maximum number of individual cells along a sandbag structure of fixed length.

Moreover, a transition model with hybrid component geometries was simulated (Supp-Fig 1D). Adverse pressure profile resulted from the mismatched

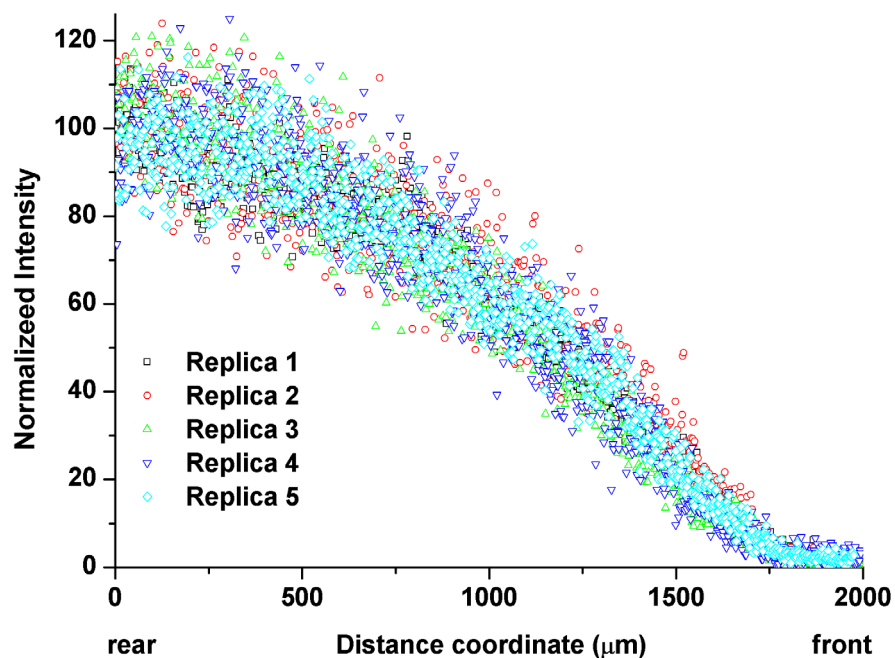
geometries between gradient and docking components was observed: (Left) Layout of transition model, a V-T hybrid and (Right) corresponding  $\Delta P_{ac}$  profile at loading and running LLP. It should be noted from the sign of  $\Delta P_{ac}$  that docking flow was reversed along the sandbag component. The pressure profile indicated that full docking was intrinsically prohibited in such hybrid design. Except for the core geometry, other parameters were comparable with T and V cores in this simulation. As mismatched geometries between gradient and docking components were not capable to sustain a low  $\Delta P_{ac}$  at running LLP, thus the design was not exemplified.

**Supplementary Figure 2: Data reproducibility on T and V shaped microdevices.**

**A**

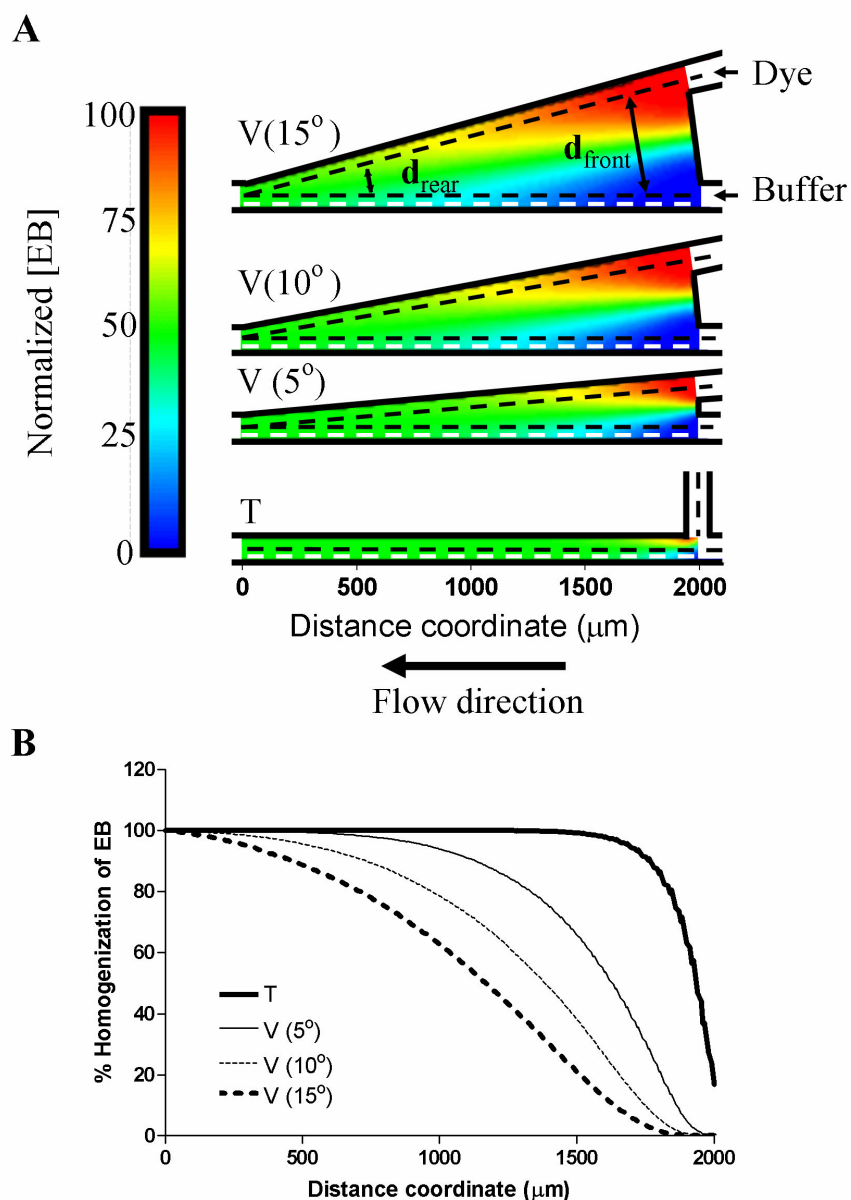


**B**



To verify the data reproducibility of T and V microdevices, EB gradient test was repeated 5 times in five PDMS microdevice replicas molded from the identical PCB master. For each microdevice, corresponding model gradient profile was identical to that shown in Fig 2B, chart of the manuscript.

**Supplementary Figure 3: Effects of geometric modulation on gradient profile.**



During microfluidic operations concerning fragile biological cells, fluidic stress should be kept at minimal<sup>2-4</sup>. While it is possible to maintain minimal stress by driving microfluidic device at slow flow rate, diffusive mixing becomes rapid in this flow rate regime, which may not be desirable for generating gradient concentrations. Equation 2 describes the mixing length required for homogenization<sup>5</sup>:

$$\text{Mixing length} \sim U \frac{I^2}{D} \quad (2)$$

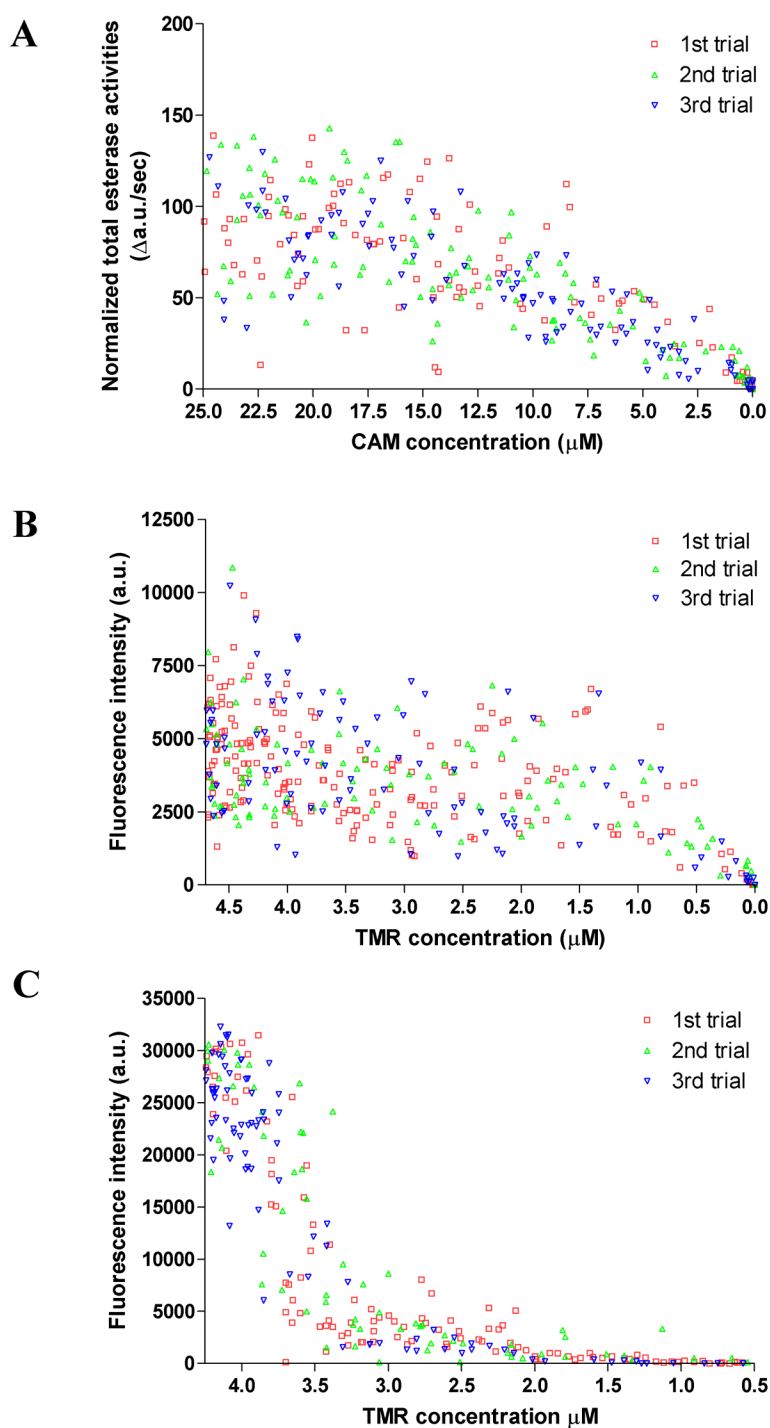
where  $U$  = average flow speed,  $I$  = cross-sectional dimension and  $D$  = molecular diffusivity. The longer the mixing length, the more gradient concentrations are

distributed over the distance along a microchannel. Although increasing  $U$  may extend the mixing length, it also creates larger stress for biological cells. By modifying  $I$ , however, it is possible to extend the mixing length without detrimental impact on cells. Therefore, gradient concentrations were increased by enlarging the width of microfluidic channel in this study.

Based on computational fluid dynamics, the geometric effects on mixing length and gradient profile were simulated using ethidium bromide (EB, diffusion coefficient:  $4.15 \times 10^{-10} \text{ m}^2\text{s}^{-1}$ ) as the model molecule. As depicted in Supp-Fig 2A, a conventional T-shaped structural model was modulated by enlarging the channel dimension near the inlet in order to create various models with V-shaped geometries. From each contour, EB gradient profile was interrogated along the white dotted line and data was plotted in Supp-Fig 2B. At identical flow rate, mixing length was significantly shorter in T ( $< 500 \text{ }\mu\text{m}$ ) than other V-shaped structures where the geometric modulation helped to distribute analyte gradient over the distance along microchannel (Supp-Table 1). Moreover, the characteristic gradient profiles among various V-shaped structures suggested the flexibility to control gradient profile and mixing length by the degree of acute angles in V-shaped microchannels.

The effect of partially enlarged V-shaped geometries could be elucidated with the term, diffusion dimension<sup>7</sup> –  $\mathbf{d}$ . In contrast to the fixed  $\mathbf{d}$  in the T-shaped structure, diffusion dimension in V-shaped structure was of variable lengths from the inlet to outlet. Confined by the V-shaped geometry, identical analyte molecules were forced to travel a longer distance to reach the interrogation line at  $\mathbf{d}_{\text{front}}$  than  $\mathbf{d}_{\text{rear}}$ , resulting in gradient profiles adjustable through the degree of acute angles.

**Supplementary Figure 4: Repeated experiments in different cell-based assays.**



The result triplicates of different on-chip cell-based assays: Supp-Fig 4A showed the trials of calcein-AM kinetic profiles that were corresponded to Fig 3C in the manuscript. Supp-Fig 4B was the TMR signal response of cells under superimposed gradient concentrations of TMR and CAM. The results was corresponded to the lower sandbag in Fig 4B. Supp-Fig 4C showed the photodynamic response of cells

after concurrently subjected to 3 minute irradiation and gradient concentrations of TMR. The result was corresponded to the upper sandbag in Fig 5B.

**Table Supplementary 1. Gradient characteristics and mixing length in differently shaped gradient components**

% Homogenization	Mixing length <sup>f</sup> (μm) required to reach % homogenization in gradient components of differently shaped microchannels			
	T	V5°	V10°	V15°
1	NIL	40	90	160
25	10	220	390	540
50	70	370	620	840
95	300	1060	1490	1720

<sup>f</sup>Distance away from the uppermost mixing point, i.e. at 2000μm



## References

1. White F. *Viscous Fluid Flow*. Boston, McGraw-Hill, 1991.
2. J. Yang, C. W. Li, M. S. Yang, *Lab on A Chip*, 2004, **4**, 53.
3. M. S. Yang, C. W. Li, J. Yang, *Analytical Chemistry*, 2002, **74**, 3991.
4. M. S. Yang, J. Yang, C. W. Li, J. L. Zhao, *Lab on A Chip*, 2002, **2**, 158.
5. A. D. Stroock, S. K. W. Dertinger, A. Ajdari, I. Mezic, H. A. Stone, G. M. Whitesides, *Science*, 2002, **295**, 647.
6. W. H. Gmeiner, C. J. Hudalla, A. M. Soto, L. Marky, *FEBS Lett.*, 2000, **465**, 148.
7. A. E. Kamholz, B. H. Weigl, B. A. Finlayson, P. Yager, *Analytical Chemistry*, 1999, **71**, 5340.